AGU PUBLICATIONS

Geophysical Research Letters

RESEARCH LETTER
10.1002/2016GL071201

Inherited crustal deformation along the East Gondwana margin revealed by seismic anisotropy tomography

S. Pilia[1], P. Arroucau[2], N. Rawlinson[3], A. M. Reading[4], and R. A. Cayley[5]

[1]Department of Petroleum Geosciences, Petroleum Institute, Abu Dhabi, United Arab Emirates, [2]Geophysics Section, School of Cosmic Physics, Dublin Institute for Advanced Studies, Dublin, Ireland, [3]School of Geosciences, University of Aberdeen, Aberdeen, UK, [4]School of Earth Sciences, Institute for Marine and Antarctic Studies and CODES Centre of Excellence, University of Tasmania, Hobart, Tasmania, Australia, [5]Geological Survey of Victoria, Melbourne, Victoria, Australia

Key Points:
- Paleofracturing trend of failed rifting between Australia and Antarctica is recorded in the anisotropy pattern
- Fast anisotropy directions exhibit a close match with magnetic lineaments and tectonic trends
- Anisotropy directions provide strong support to recent geodynamic and kinematic modeling results that address continental accretion

Supporting Information:
- Supporting Information S1

Correspondence to:
S. Pilia,
spilia@pi.ac.ae

Citation:
Pilia, S., P. Arroucau, N. Rawlinson, A. M. Reading, and R. A. Cayley (2016), Inherited crustal deformation along the East Gondwana margin revealed by seismic anisotropy tomography, *Geophys. Res. Lett.*, *43*, 12,082–12,090, doi:10.1002/2016GL071201.

Received 20 SEP 2016
Accepted 22 NOV 2016
Accepted article online 25 NOV 2016
Published online 15 DEC 2016

Abstract The mechanisms of continental growth are a crucial part of plate tectonic theory, yet a clear understanding of the processes involved remains elusive. Here we determine seismic Rayleigh wave phase anisotropy variations in the crust beneath the southern Tasmanides of Australia, a Paleozoic accretionary margin. Our results reveal a complex, thick-skinned pervasive deformation that was driven by the tectonic interaction between the proto-Pacific Ocean and the ancient eastern margin of Gondwana. Stress-induced effects triggered by the collision and entrainment of a microcontinent into the active subduction zone are evident in the anisotropy signature. The paleofracturing trend of failed rifting between Australia and Antarctica is also recorded in the anisotropy pattern as well as a tightly curved feature in central Tasmania. The observed patterns of anisotropy correlate well with recent geodynamic and kinematic models of the Tasmanides and provide a platform from which the spatial extent of deformational domains can be refined.

1. Introduction

Isotropic tomographic models often exhibit features that are difficult to explain or are inconsistent with constraints supplied by independent data sets (e.g., geochemical, surface mapping, and geochronology). In many cases, regardless of the level of data fit, unexpected velocity perturbations can be explained by invoking seismic anisotropy [*Babuska and Cara*, 1991]. In general terms, seismic anisotropy describes the directional dependence of seismic wave speeds, in contrast to the assumption of isotropic velocity variations, which are invariant with respect to direction. Regular patterns of tectonic fabric, stress-aligned microcracks, and preferred mineral alignment are typically invoked to explain seismic anisotropy in crustal studies [*Babuska and Cara*, 1991; *Crampin*, 1994]. With appropriate data sets, crustal seismic anisotropy can be mapped with good resolution at local-regional scale to search for evidence of present-day deformation and past deformation events “frozen” into the tectonic fabric, which can supply important constraints to dynamic and kinematic models [*Fry et al.*, 2010; *Rawlinson et al.*, 2014].

Major accretionary orogens such as the Altaids or the northern Appalachians are the final product of convergent margin tectonism that promotes significant crustal growth at the boundaries of continental landmasses. The Phanerozoic Tasmanides of eastern Australia is one of the largest and most complete examples of accretionary orogens in existence and has been the main proving ground for the development of a new geodynamic model that provides crucial insights into continental growth [*Cayley*, 2012; *Moresi et al.*, 2014]. The Tasmanides evolved from the tectonic interaction between the proto-Pacific Ocean and the eastern supercontinent Gondwana, along which continental material was progressively accreted onto the Precambrian margin of western and central Australia from the Neoproterozoic to the Jurassic [*Glen*, 2013]. Its expression in today’s geology is characterized by a complex amalgamation of multiple orogeny-parallel accretionary events, embedment of exotic continental blocks, large oroclines, and several arc complexes. Models that attempt to assess the evolution of the southern Tasmanides (Figure 1), which comprises the Lachlan Fold Belt, are contentious and often inadequately fit paleogeographic and timing constraints [*Foster and Gray*, 2000; *Fergusson*, 2010; *Cayley*, 2011]. Observational constraints of the preserved crustal structures are minimal as they are largely buried under Mesozoic and Cainozoic terranes and, perhaps more importantly, strongly reworked and overprinted by protracted successions of tectonomagmatic events that affected the region

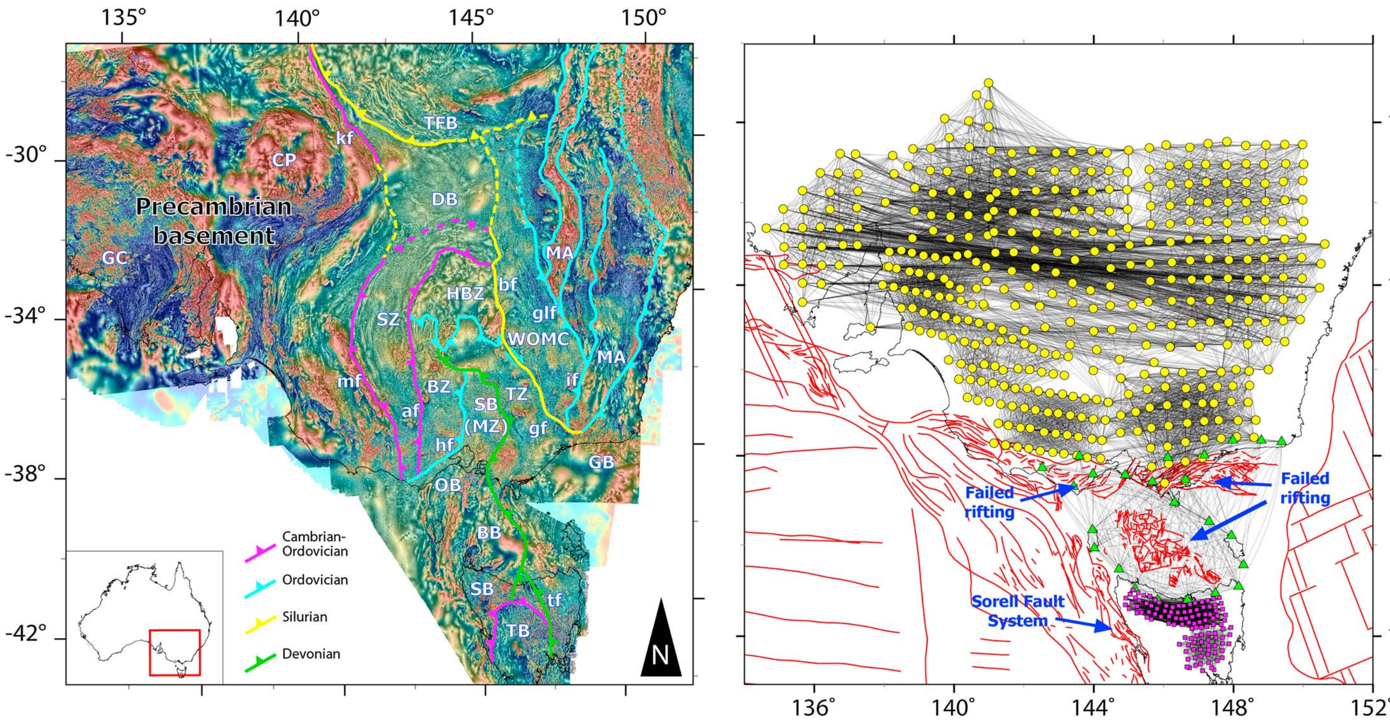

Figure 1. (left) Background image shows tilt-filtered TMI map, using data from the 2010 compilation of Australian aeromagnetic data provided by Geoscience Australia, decimated to a 250 m grid. The spectrum from blue to red indicates variations of the tilt angle from +90° to −90°. The tilt angle is positive (red) over magnetic sources, close to zero (yellow/green) when at the edge of the source, and negative (blue) when away from it (see section 3 for further details). Major tectonic boundaries are outlined [after *Moresi et al.*, 2014; *Pilia et al.*, 2015a]. Different colors represent different boundary ages. GC: Gawler Craton; CP: Curnamona Province; TFB: Thomson Fold Belt; DB: Murray-Darling Basin; SZ: Stawell Zone (Lachlan Orocline); HBZ: Hay-Booligal Zone; BZ: Bendigo Zone; SB: Selwyn Block beneath Melbourne Zone (MZ); WOMC: Wagga-Omeo Metamorphic Complex; MA: Macquarie Arc; OT: Otway Basin; BB: Bass Basin; GB: Gippsland Basin; TB: Tyennan Block. mf: Moyston Fault; kf: Koonenberry Fault; af: Avoca Fault; hf: Heathcote Fault; gf: Governor Fault; bf: Bootheragandra Fault; if: Indi Fault; glf: Gilmore Fault Zone; tf: Tamar Fracture System. The Lachlan Fold Belt comprises the tectonic bodies east of the Moyston Fault and south of the Thomson Fold Belt. (right) The raypath coverage at 8 s period showing the irregular spatial distribution of data among the three main deployments (yellow circles are stations in mainland Australia, and green triangles and magenta squares are, respectively, from Bass Strait and Tasmania). Stations of the 11 subarrays in mainland Australia have an interstation space of approximately 50 km, much larger than that found in Tasmania (about 15 km). Red lines represent the main tectonic elements (inferred from shallow seismic reflection profiles and magnetic anomalies) resulting from the separation of Australia and Antarctica.

(e.g., Australia-Antarctica breakup, Quaternary Newer Volcanic Province intraplate volcanism, and uplift of the Southern Highlands) [*Weissel and Hayes*, 1972; *Wellman*, 1974; *Lambeck and Stephenson*, 1986]. An additional challenge is provided by the allochthonous lithologies of western Tasmania, which have no apparent along-strike relationship to the larger-scale history of mainland Australia. Tomographic studies performed during the last two decades have progressively contributed toward defining the 3-D extent of the building blocks characterizing the southern Tasmanides by assuming isotropic velocity variations. For example, *Pilia et al.* [2015a] recently produced a 3-D shear velocity model of the southern Tasmanides (including Bass Strait and Tasmania) which provided direct evidence for the existence of the main tectonic elements as postulated by the geodynamic models of *Cayley et al.* [2002] and *Moresi et al.* [2014]. On a larger scale, *Rawlinson et al.* [2015] was able to illuminate the crust-mantle system beneath southern mainland Australia by inverting teleseismic arrival times and including a detailed crustal model derived from ambient noise tomography. Nonetheless, the dynamics that forged this vast orogenic collage are yet to achieve a widespread consensus and are still hotly debated.

Recent developments in ambient noise tomography, coupled with the availability of large passive data sets from dense arrays, provide the exciting possibility of extracting detailed information on azimuthal anisotropy. In this paper we use continuous ambient noise recordings that mainly originate from oceanic disturbances to investigate the crust beneath mainland southeast Australia, Bass Strait, and Tasmania and account for the apparent azimuthal dependence of measured Rayleigh wave phase velocities. Equipped with this additional information, our primary aim is to relate crustal anisotropy to the regional tectonics and shed new light on the evolution of the entire southern Tasmanides.

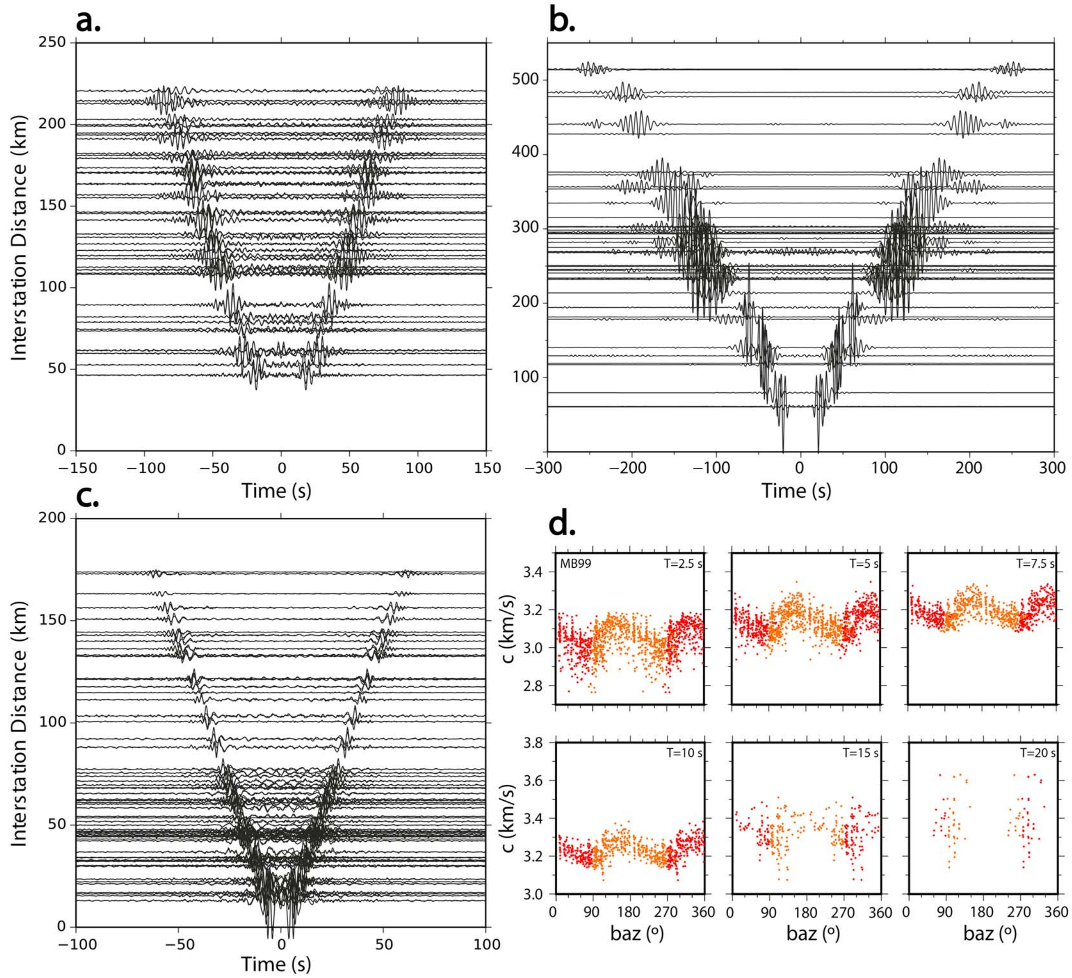

Figure 2. Three examples of long-term cross correlations using data from different WOMBAT subarrays: (a) mainland Australia, (b) Bass Strait, and (c) Tasmania. A Butterworth filter with corner frequencies 0.03 and 2 Hz has been applied before the computation of cross correlations. All amplitudes are multiplied by a factor to enhance visualization at longer distances. (d) Relationship between Rayleigh phase velocities and back azimuth for the subarray MB99 (located west of the southern Moyston Fault). Clear 180° periodicity is observed at most periods. The paucity of data above $T = 15$ s period makes it difficult to identify the same pattern at longer periods.

2. Methods and Results

Data for this study are sourced from 582 stations (Figure 1) of the high-density WOMBAT transportable seismic array, which has a station spacing of approximately 15 and 50 km in Tasmania and mainland Australia, respectively. This array has been operating in southeast Australia since 1998 and has been progressively moved 16 times. Recording periods vary from a minimum of 4 months to a maximum of about 18 months. We have computed nearly 15,000 empirical Green's functions (EGFs) by cross-correlating 1 h segments of all the simultaneously recording station pairs, as described in *Arroucau et al.* [2010] (see Text S1 in the supporting information for a more detailed discussion) [*Shapiro and Campillo*, 2004; *Bensen et al.*, 2007]. For the stations around Bass Strait, where the signal-to-noise ratio was poorest, the time domain phase-weighted stacking algorithm of *Schimmel et al.* [2011] was employed, which significantly improved the quality of the EGFs (Figure 2; see also Text S1 and Figure S1). Rayleigh wave phase velocity measurements were then extracted from the cross correlograms of the vertical component of all station pairs using the method described by *Young et al.* [2013a]; this resulted in path-averaged phase velocities for periods ranging from 2 to 20 s (see Text S2 and Figures S1 and S2) [*Yao et al.*, 2006]. To initially evaluate the period dependency of seismic anisotropy in our data set, we plot the interstation phase velocities against the back azimuth between station pairs of the subarray MB99 (western southeastern Australia, Figure 2). From this subarray, as well as the majority in the region (Figures S3 and S4), a dominant signal with 180° periodicity is observed at most periods, which is

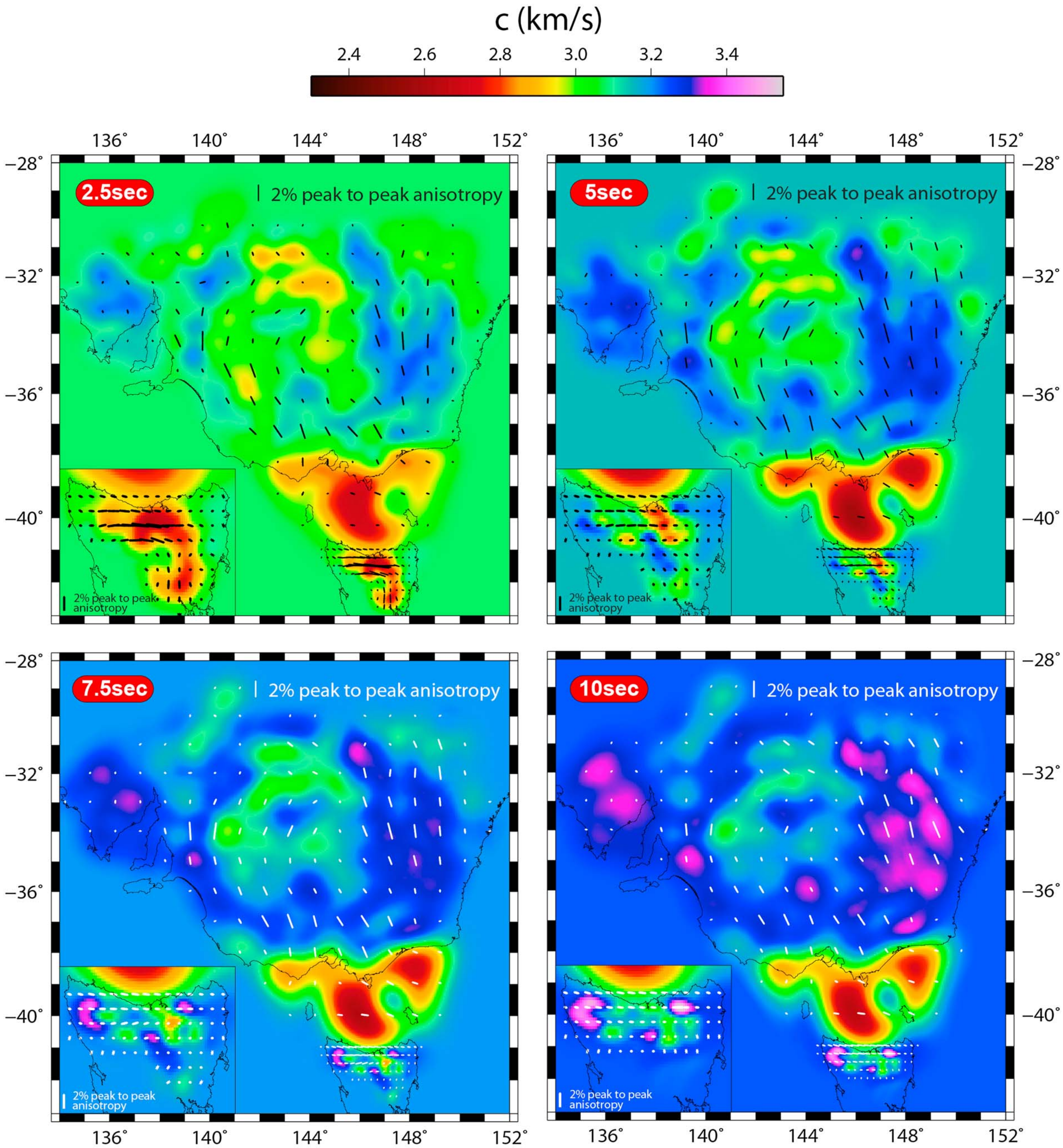

Figure 3. Final 2-D phase velocity maps as a function of period (2.5, 5, 7.5, and 10 s) illustrating both the isotropic and anisotropic components of the wavefield in southeastern Australia. The color bar scale indicates the absolute variation of the isotropic velocity field, while the black (top) and white (bottom) bars show the peak-to-peak anisotropy. The length of the bars is proportional to the magnitude of anisotropy, and the direction is aligned with the fast axis of anisotropy. Peak sensitivity of the phase velocity occurs at a depth approximately equal to the period in seconds multiplied by 1 km/s. The insets in the bottom left corners represent zoom-ins of Tasmania taken from 144.5°/−40.5° (top left) and 148.5°/−43.0° (bottom right).

indicative of so-called 2π azimuthal anisotropy. The emergence of this mode of anisotropy is consistent with a range of scenarios, including preferred orientation of reworked minerals after extensive metamorphism (i.e., foliation), a system of geological features (e.g., dikes and lineations), or fractures aligned in one direction [*Babuska and Cara*, 1991]. We subsequently inverted interstation traveltimes and mapped the inherited lateral phase velocity variations for both isotropic and anisotropic wavefield components over a period range of 2–20 s. To this end, we applied the surface wave tomography algorithm of *Debayle and Sambridge* [2004]. The underlying code is based on the continuous regularization algorithm of *Montagner* [1986] and accounts for the azimuthal Rayleigh wave variation through one isotropic term and four anisotropic coefficients [*Smith and Dahlen*, 1973]. However, since only 2π anisotropy is observed in the data, we ignore the two 4π coefficients [*Montagner and Nataf*, 1986]; hence, three unknowns per grid point are considered during the inversion process (see Text S3 in the supporting information). The isotropic solution model generally reduces the data variance by about 65%. When including the anisotropic terms in the inversion, the fit to the measured traveltimes is generally improved by approximately 10%. Although the isotropic component dominates the data misfit, this is suggestive of relatively significant contribution of anisotropy in the inversion.

Resolution tests based on synthetic data were carried out separately for the isotropic and anisotropic components of the wavefield by using identical source-receiver combinations to the observational data set (see Text S4 and Figures S6–S9). The spatial resolution was assessed through a predetermined checkerboard input, which involves the alternation of high- and low-velocity perturbations, as well as the alternation of fast directions of anisotropy. The quality of the recovered checkerboard pattern is generally good, with structures as small as about 20 km accurately retrieved in Tasmania in both shape and absolute amplitude. The trade-off between isotropic and anisotropic components is also well resolved, which is testament to the density and azimuthal variability of the path coverage (see Figure 1).

We present the crustal structure beneath southeastern Australia via a series of period-dependent phase velocity maps (Figure 3), in which the orientation of the fast axes of anisotropy is superimposed onto the isotropic component of the wavefield. The regional pattern of isotropic phase velocity variations is similar to previous 2-D and 3-D isotropic tomographic models based on ambient noise recordings [*Young et al.*, 2013b, 2013a; *Pilia et al.*, 2015a, 2015b]. This appears to suggest that the final isotropic tomographic models from southeastern Australia are not significantly affected by the addition of azimuthal anisotropy to the inversion process. A prominent feature of the isotropic velocity distribution maps is the correspondence of the low-velocity areas with sedimentary basins, such as the Murray-Darling Basin in mainland Australia and the Otway, Bass, and Gippsland basins in Bass Strait (see Figures 1 and S10 for exact location of sedimentary basins). In terms of azimuthal anisotropy, there is little change in pattern as a function of depth in the crust, suggesting that it may not be stratified but could instead have the same origin. Given the consistency of the anisotropy signature with magnetic observations as we show below, it is then possible that the crust is rather uniform over large depths. Of particular relevance to further discussion is the major transition in the fast axes direction as defined by a counterclockwise rotation of more than 90° observed when entering Bass Strait from mainland Australia. Furthermore, we find that both anisotropy directions and magnetic response make a remarkable match with what *Cayley* [2015] postulates to be an isoclinal orocline in Tasmania.

3. Discussion

Total magnetic intensity anomalies can be used to constrain the composition and tectonic fabric lineaments of the crust where temperatures are below the Curie point. Thus, it is useful to compare the anisotropy tomography results with a magnetic map [*Bokelmann and Wüstefeld*, 2009; *Rawlinson et al.*, 2014], which may help explain the origin of the anisotropy within the WOMBAT array. Variable thicknesses of post-Paleozoic cover, which exceeds 5 km in parts of the Darling Basin and 10 km in Bass Strait, make upper crustal structure difficult to recognize in conventional presentations of aeromagnetic data. The tilt filter is a phase filter defined as the ratio between the first derivative of the potential field and the horizontal gradient of the field [*Miller and Singh*, 1994], and it is expressed as a tilt angle. When applied to total magnetic intensity (TMI), it yields imagery that traces geological structure over a wide range in dynamic signal and depth of source [*Cooper and Cowan*, 2006]. In Figure 4 we have superimposed the fast anisotropy axis computed at 2.5 and 5 s period onto a tilt-filtered magnetic intensity image. It is worth noting that our ability to make inferences about the tectonic events that shaped the region is limited to the last event of substantial deformation, which remains frozen in the crust and produces the observed anisotropy. An additional challenge is to determine which tectonic event may have generated a specific anisotropic pattern, since more than one type of deformational episode may produce the same orientation of anisotropy.

Rawlinson et al. [2014] recently presented new azimuthal tomography results from Rayleigh wave phase velocity variations in mainland Australia. They compared the orientation of magnetic fabric with the fast axis of anisotropy and found compelling corroboration for the 3-D geodynamic model of *Moresi et al.* [2014]. In their paper, *Moresi et al.* [2014] address the evolution of accretionary orogens through sophisticated 3-D numerical modeling, predicting how the ingestion of drifting continental blocks may result in prominent curvature of

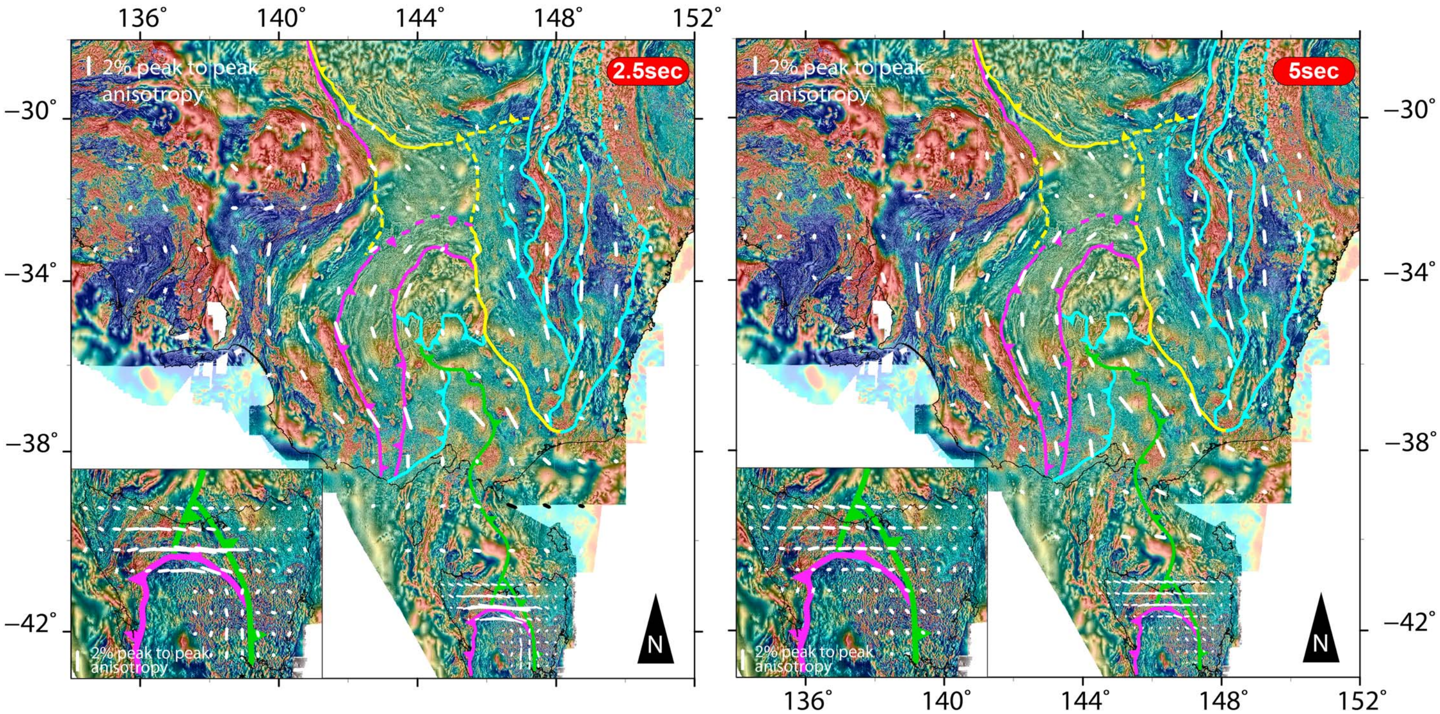

Figure 4. Comparison of the tilt-filtered magnetic map with the orientation of the fast axes of seismic anisotropy from the 2.5 and 5 s period maps. Colors and tectonic boundaries are as per Figure 1. A remarkable correlation between the orientation of magnetic fabric and the fast axes of anisotropy is revealed in mainland Australia and Tasmania. The insets in the bottom left corners represent zoom-ins of Tasmania taken from 144.5°/−40.5° (top left corner) and 148.5°/−43.0° (bottom right corner).

orogenic systems, as well as tectonic escape of the back-arc region during subduction congestion and subsequent reestablishment of a stable convergent margin. Perhaps the most profound finding that emerged from the study of *Rawlinson et al.* [2014], also discernible in Figures 3 and 4, is the delineation by the fast anisotropy axis of a strongly curved region. This mimics a distinct belt of deeply sourced (minimum depth to top is between 1 and 5 km) magnetic highs, which coincides with the Cambrian Stawell Zone and appears to be overprinted by a giant orocline (Lachlan Orocline, Figures 1 and 4). However, *Rawlinson et al.* [2014] did not cover Tasmania or Bass Strait, which encompass a significant part of the orogenic system and geodynamic model. Thus, we predominantly focus on attributes that arise in Bass Strait and Tasmania, with emphasis on larger-scale implications for the southern Tasmanides.

Evidence of the geodynamic model computed by *Moresi et al.* [2014] for the Tasmanides is weak in Bass Strait and somewhat equivocal in northern Tasmania, as more recent deformational events have possibly reworked previous anisotropy imprints. Heading south into Bass Strait from Victoria, both the strength and orientation of anisotropy change significantly (Figures 3 and 4), and the remarkable correlation seen in mainland Australia with the magnetic lineaments seems to be lost, although we note that our ability to retrieve a strong anisotropy signature may be reduced by the lower signal-to-noise ratio of the Bass Strait data set. In order to better understand this pattern, we must consider both the magnetic anomalies and tectonic blocks which characterize Bass Strait. The western part of Bass Strait comprises three continuous metavolcanic Cambrian-Proterozoic belts with strong magnetic signatures that can be traced without major disruption from northwestern Tasmania to Victoria and are thought to be part of the exotic Proterozoic microcontinent called Selwyn Block [*Cayley et al.*, 2002; *Cayley*, 2011]. The central region is marked by a large high magnetic anomaly underlying Bass Basin (40° S and 146.5° E), whereas the eastern region has a structurally distinct and weak magnetic signature with a granite-turbidite fabric. One major cycle of tectonic activity that affected this area through extension and subsidence is the breakup between Australia and Antarctica, along the so-called Southern Margin Rift System. This began at about 90–87 Ma off the southern Naturaliste Plateau (offshore western Australia) and propagated as a diachronous event from west to east [*Direen*, 2012]. By the end of the Cretaceous, the rift system penetrated Bass Strait but failed to find a lithospheric weakness that could successfully accommodate a separation between Tasmania and Australia. Two failed arms were created in Bass Strait

(Otway and Gippsland basins and subsequently Bass Basin), which produced a topographic low that received sediments for the three basins we observe today. Breakup continued and eventually ceased along the Sorell fault system off the western Tasmanian coast (Figure 1). The pattern of anisotropy in eastern and central Bass Strait induced by this tectonic event is likely to be parallel to the fracturing of the upper crust that occurred in directions broadly orthogonal to the northeast-southwest tension forces resulting from the failed rifts [*Kendall et al.*, 2006]. In support of this hypothesis, the orientation of the fast anisotropy axes here, particularly at 5 s period, is congruent with the strike of the deep igneous body beneath Bass Basin (40°S and 146.5°E). Its geometry suggests that magma emplacement might have been controlled by northeasterly extension, with the intrusion being generated as extension progressed and then terminated when the breakup failed [*Gunn et al.*, 1997; *Müller et al.*, 2012]. This pattern of anisotropy is in stark contrast with that observed in adjacent mainland Australia but appears to partially propagate into northern Tasmania. Intriguingly, the western part of Bass Strait exhibits an approximately N-S fast axis of anisotropy, which becomes stronger with increasing period (Figures 3 and 4). Even though this may appear to be a continuation of the same trend from mainland Australia (i.e., Bendigo and Stawell zones), the strong correlation with the north trending magnetic belts from western Tasmania to Victoria suggests that it may be inherited from the Selwyn block (SB in Figure 1). We also speculate that as the continental ribbon behaved as a rigid block, the spreading occurring between Australia and Antarctica was forced to propagate along another viable path (Sorell fault system), preventing deformation of the Selwyn Block and retaining a substantially intact pattern of anisotropy from the Mesoproterozoic [*Cayley*, 2011].

Further south in Tasmania, the pattern of anisotropy exhibits a strong correlation with the magnetic lineaments albeit mostly limited to periods of 2.5 and 5 s. In the core of Tasmania, the fast anisotropy axis traces out a strongly arcuate trend, which approximately coincides with an abrupt west-east transition from high to low isotropic phase velocities. Evidence of this also comes from the magnetic map, as the Tyennan Block stands out as predominantly composed of nonmagnetic Proterozoic rocks. The northern end of this discrete feature coincides with the position of the so-called "Dundas-Fossey Arc," a region of curved Cambrian rocks that extends east from the Dundas Trough in western Tasmania [*Corbett and Turner*, 1989]. *Cayley* [2015] has interpreted this feature as part of a larger isoclinal oroclinal fold formed in the Early Devonian. The eastern extent of this orocline is largely concealed beneath younger cover but is clearly revealed in the fast anisotropy axis traces. The correlation between the preserved anisotropic signature and the magnetic lineaments in the upper crust supports the idea that the rock record has retained a pattern that dates back to the time of deformation in the Paleozoic. To provide a geodynamic link to the model of *Moresi et al.* [2014] in Tasmania, *Cayley* [2015] proposes that the orocline was partially created during the Bindian Orogeny (Early Devonian) as the Selwyn Block is entirely embedded in the overriding plate and slab rollback propagates asymmetrically, transferring material behind the continental ribbon. East-west compression during the Tabberabberan Orogeny (Middle Devonian) acted to finally tighten the orocline. One caveat with our results in Tasmania is that the amplitude of anisotropy rapidly decreases with period, particularly above 5 s, as does the presence of a coherent pattern of anisotropy (Figure 3); this is due to the limited aperture of the Tasmanian arrays, which limits the maximum period (hence depth) that can be exploited and, to a lesser extent, the higher levels of data noise that are present at longer periods due to the use of short-period (1 Hz) seismometers.

4. Conclusions

Period-dependent variations of Rayleigh wave phase azimuthal anisotropy are extracted from continuous ambient noise records to investigate crustal deformation in the Tasmanides orogenic system of southeastern Australia. Comparison of the anisotropy pattern with existing high-resolution aeromagnetic data and regional tectonic trends reveals a compelling degree of consistency. Our results are compatible with recent geodynamic modeling that addresses continental accretion in the ancient eastern margin of Gondwana as affected by the entrainment of a microcontinent and are useful in delineating the spatial extent of regional deformational domains. The close match of the magnetic lineaments and the directions of anisotropy in central Tasmania is a record of pervasive deformation that supports the existence of a tight orocline within western Tasmania. Failed rifting in central and eastern Bass Strait associated with the breakup between Australia and Antarctica appears to have reworked prior anisotropy signatures. Here the orientation of the fast axis of anisotropy frozen in the rock record is virtually orthogonal to the predominant direction of maximum extension in the Cretaceous.

Acknowledgments
We thank Mallory Young for providing phase velocity measurements in mainland Australia and Tasmania. Robert Musgrave is thanked for making available his tilt-filtered magnetic intensity map. In the short term, data may be made available by contacting the authors (S.P. or N.R.). A new database of passive seismic data recorded in Australia is planned as part of a national geophysics data facility for easy access download. Details on the status of this database may be obtained from the authors (S.P., N.R., or A.M.R.). There are no restrictions on access for noncommercial use. Commercial users should seek written permission from the authors (S.P. or N.R.). Ross Cayley publishes with the permission of the Director of the Geological Survey of Victoria.

References

Arroucau, P., N. Rawlinson, and M. Sambridge (2010), New insight into Cainozoic sedimentary basins and Palaeozoic suture zones in southeast Australia from ambient noise surface wave tomography, *Geophys. Res. Lett.*, *37*, L07303, doi:10.1029/2009GL041974.

Babuska, V., and M. Cara (1991), *Seismic Anisotropy in the Earth*, vol. 10, Springer, Netherlands.

Bensen, G. D., M. H. Ritzwoller, M. P. Barmin, A. L. Levshin, F. Lin, M. P. Moschetti, N. M. Shapiro, and Y. Yang (2007), Processing seismic ambient noise data to obtain reliable broad-band surface wave dispersion measurements, *Geophys. J. Int.*, *169*(3), 1239–1260, doi:10.1111/j.1365-246X.2007.03374.x.

Bokelmann, G. H., and A. Wüstefeld (2009), Comparing crustal and mantle fabric from the North American craton using magnetics and seismic anisotropy, *Earth Planet. Sci. Lett.*, *277*(3), 355–364, doi:10.1016/j.epsl.2008.10.032.

Cayley, R., D. Taylor, A. VandenBerg, and D. Moore (2002), Proterozoic-early Palaeozoic rocks and the Tyennan orogeny in central Victoria: The Selwyn Block and its tectonic implications, *Aust. J. Earth Sci.*, *49*(2), 225–254, doi:10.1046/j.1440-0952.2002.00921.x.

Cayley, R. A. (2011), Exotic crustal block accretion to the eastern Gondwanaland margin in the Late Cambrian-Tasmania, the Selwyn Block, and implications for the Cambrian-Silurian evolution of the Ross, Delamerian, and Lachlan orogens, *Gondwana Res.*, *19*(3), 628–649, doi:10.1016/j.gr.2010.11.013.

Cayley, R. A. (2012), Oroclinal folding in the Lachlan Fold Belt: Consequence of southeast-directed Siluro-Devonian subduction rollback superimposed on an accreted Ordovician arc assemblage in eastern Australia, *Geol. Soc. Aust. Extended Abst.*, *103*, 34–43.

Cayley, R. A. (2015), A new geodynamic model for Cambrian Tasmania/Australian East Gondwanaland—Continent-continent collision above doubly divergent Dundas Trough subduction zones, in *Riding the Wave: GSA Specialist Group in Tectonics and Structural Geology Conference*, edited by R. A. Cayley, pp. 21–22, Geol. Soc. of Aust., Hornsby, NSW, Australia.

Cooper, G., and D. Cowan (2006), Enhancing potential field data using filters based on the local phase, *Comput. Geosci.*, *32*(10), 1585–1591, doi:10.1016/j.cageo.2006.02.016.

Corbett, K., and N. Turner (1989), Early Palaeozoic deformation and tectonics, in *Geology and Mineral Resources of Tasmania*, edited by K. Corbett and N. Turner, pp. 154–181, Spec. Publ. Geol. Soc. of Aust., Hornsby, NSW, Australia.

Crampin, S. (1994), The fracture criticality of crustal rocks, *Geophys. J. Int.*, *118*(2), 428–438, doi:10.1111/j.1365-246X.1994.tb03974.x.

Debayle, E., and M. Sambridge (2004), Inversion of massive surface wave data sets: Model construction and resolution assessment, *J. Geophys. Res.*, *109*, B02316, doi:10.1029/2003JB002652.

Direen, N. (2012), Comment on "Antarctica—Before and after Gondwana" by S.D. Boger Gondwana Research, Volume 19, Issue 2, March 2011, pages 335–371, *Gondwana Res.*, *21*(1), 302–304, doi:10.1016/j.gr.2011.08.008.

Fergusson, C. L. (2010), Plate-driven extension and convergence along the East Gondwana active margin: Late Silurian–Middle Devonian tectonics of the Lachlan Fold Belt, southeastern Australia, *Aust. J. Earth Sci.*, *57*(5), 627–649, doi:10.1080/08120099.2010.494767.

Foster, D. A., and D. R. Gray (2000), Evolution and structure of the Lachlan Fold Belt (Orogen) of eastern Australia, *Annu. Rev. Earth Planet. Sci.*, *28*(1), 47–80, doi:10.1146/annurev.earth.28.1.47.

Fry, B., F. Deschamps, E. Kissling, L. Stehly, and D. Giardini (2010), Layered azimuthal anisotropy of Rayleigh wave phase velocities in the European Alpine lithosphere inferred from ambient noise, *Earth Planet. Sci. Lett.*, *297*(1), 95–102, doi:10.1016/j.epsl.2010.06.008.

Glen, R. A. (2013), Refining accretionary orogen models for the Tasmanides of eastern Australia, *Aust. J. Earth Sci.*, *60*(3), 315–370, doi:10.1080/08120099.2013.772537.

Gunn, P., T. Mackey, A. Yeates, R. Richardson, D. Seymour, M. McClenaghan, C. Calver, and M. Roach (1997), The basement elements of Tasmania, *Exploration Geophys.*, *28*(2), 225–231, doi:10.1071/EG997225.

Kendall, J.-M., S. Pilidou, D. Keir, I. Bastow, G. Stuart, and A. Ayele (2006), Mantle upwellings, melt migration and the rifting of Africa: Insights from seismic anisotropy, *Geol. Soc. London Spec. Publ.*, *259*(1), 55–72, doi:10.1144/GSL.SP.2006.259.01.06.

Lambeck, K., and R. Stephenson (1986), The post-Palaeozoic uplift history of south-eastern Australia, *Aust. J. Earth Sci.*, *33*(2), 253–270, doi:10.1080/08120098608729363.

Miller, H. G., and V. Singh (1994), Potential field tilt—A new concept for location of potential field sources, *J. Appl. Geophys.*, *32*(2), 213–217, doi:10.1016/0926-9851(94)90022-1.

Montagner, J. (1986), Regional three-dimensional structures using long-period surface waves, *Ann. Geophys.*, *4*(B3), 283–294.

Montagner, J.-P., and H.-C. Nataf (1986), A simple method for inverting the azimuthal anisotropy of surface waves, *J. Geophys. Res.*, *91*(B1), 511–520, doi:10.1029/JB091iB01p00511.

Moresi, L., P. Betts, M. Miller, and R. Cayley (2014), Dynamics of continental accretion, *Nature*, *508*(7495), 245–248, doi:10.1038/nature13033.

Müller, R., S. Dyksterhuis, and P. Rey (2012), Australian paleo-stress fields and tectonic reactivation over the past 100 Ma, *Aust. J. Earth Sci.*, *59*(1), 13–28, doi:10.1080/08120099.2011.605801.

Pilia, S., N. Rawlinson, R. Cayley, T. Bodin, R. Musgrave, A. Reading, N. Direen, and M. Young (2015a), Evidence of micro-continent entrainment during crustal accretion, *Sci. Rep.*, *5*, 8218, doi:10.1038/srep08218.

Pilia, S., N. Rawlinson, N. Direen, A. Reading, R. Cayley, L. Pryer, P. Arroucau, and M. Duffett (2015b), Linking mainland Australia and Tasmania using ambient seismic noise tomography: Implications for the tectonic evolution of the east Gondwana margin, *Gondwana Res.*, *28*(3), 1212–1227, doi:10.1016/j.gr.2014.09.014.

Rawlinson, N., P. Arroucau, R. Musgrave, R. Cayley, M. Young, and M. Salmon (2014), Complex continental growth along the proto-Pacific margin of East Gondwana, *Geology*, *42*(9), 783–786, doi:10.1130/G35766.1.

Rawlinson, N., S. Pilia, M. Young, M. Salmon, and Y. Yang (2015), Crust and upper mantle structure beneath southeast Australia from ambient noise and teleseismic tomography, *Tectonophysics*, *689*, 143–156, doi:10.1016/j.tecto.2015.11.034.

Schimmel, M., E. Stutzmann, and J. Gallart (2011), Using instantaneous phase coherence for signal extraction from ambient noise data at a local to a global scale, *Geophys. J. Int.*, *184*(1), 494–506, doi:10.1111/j.1365-246X.2010.04861.x.

Shapiro, N. M., and M. Campillo (2004), Emergence of broadband Rayleigh waves from correlations of the ambient seismic noise, *Geophys. Res. Lett.*, *31*, L07614, doi:10.1029/2004GL019491.

Smith, M. L., and F. Dahlen (1973), The azimuthal dependence of Love and Rayleigh wave propagation in a slightly anisotropic medium, *J. Geophys. Res.*, *78*(17), 3321–3333, doi:10.1029/JB078i017p03321.

Weissel, J. K., and D. E. Hayes (1972), Magnetic anomalies in the southeast Indian Ocean, in *Antarctica Oceanology II: The Australian-New Zealand Sector*, edited by D. E. Hayes, pp. 165–196, AGU, Washington, D. C.,10.1029/AR019p0165.

Wellman, P. (1974), Potassium-argon ages on the Cainozoic volcanic rocks of eastern Victoria, Australia, *J. Geol. Soc. Aust.*, *21*(4), 359–376, doi:10.1080/00167617408728858.

Yao, H., R. D. van Der Hilst, and M. V. de Hoop (2006), Surface-wave array tomography in SE Tibet from ambient seismic noise and two-station analysis: I. Phase velocity maps, *Geophys. J. Int.*, *166*(2), 732–744, doi:10.1111/j.1365-246X.2006.03028.x.

Young, M. K., R. A. Cayley, M. A. McLean, N. Rawlinson, P. Arroucau, and M. Salmon (2013a), Crustal structure of the east Gondwana margin in southeast Australia revealed by transdimensional ambient seismic noise tomography, *Geophys. Res. Lett.*, *40*, 4266–4271, doi:10.1002/grl.50878.

Young, M. K., N. Rawlinson, and T. Bodin (2013b), Transdimensional inversion of ambient seismic noise for 3D shear velocity structure of the Tasmanian crust, *Geophysics*, *78*(3), WB49–WB62, doi:10.1190/geo2012-0356.1.